Commensurate Defect Superstructures in a Langmuir-Blodgett Film

D. K. Schwartz, R. Viswanathan, and J. A. N. Zasadzinski[a]

Department of Chemical and Nuclear Engineering, University of California, Santa Barbara, California 93106

(Received 10 August 1992)

Molecular-resolution atomic force microscope images of Ba arachidate Langmuir-Blodgett multilayers show two previously unknown structures, a tilted (26°) triclinic packing with a 3×1 sawtooth height modulation, and a tilted (19°) rectangular herringbone packing with an alternating vertical offset, along with untilted disordered regions, all within the same molecular layer. The submicron extent of each region, the extent of twinning and defects, and the complexity of the molecular packing make the determination of the lattice structure of these materials impossible by any other technique.

PACS numbers: 61.16.Ch, 61.50.Jr, 61.72.Ff, 68.35.Bs

Langmuir-Blodgett (LB) films have been studied by a variety of scattering and spectroscopic techniques which provide information about average molecular order and orientation [1,2]. However, features of interest are often smaller than the minimum areas these probes can measure, and the averaging can make analysis difficult. The atomic force microscope [3] (AFM) is an essential technique for LB film characterization because of its ability to identify lattice structure and defects on length scales ranging from angstroms [4–8] to microns [9,10].

LB films of cadmium arachidate (CdA) as thin as two molecular layers show features reminiscent of bulk crystals, such as long-range order [6,7] and grain boundaries [6]. However, they also have distinctive features such as an incommensurate height modulation [6], and are sensitive to the number of layers [7,10], *p*H during deposition [9], or type of cation [8]. This is intriguing because the molecular packing, symmetry, and lattice dimensions of such systems have always been shown to correspond to one or another of the well-known packings of long-chain alkanes [6,8,11,12]. In this paper we show that the simple substitution of Ba for Cd in LB films changes the crystal structure dramatically from a uniform, untilted, noncentered rectangular herringbone lattice for Cd [6,7] to three different packing arrangements for Ba. The predominant structure (~70% of the surface area) in Ba arachidate (BaA) is a previously unknown lattice best described as a tilted, triclinic packing with a regular commensurate superstructure of packing defects resulting in a "sawtooth" surface modulation and a three-molecule unit cell of area 61.1 $Å^2$ (20.4 $Å^2$/molecule). The effect of the packing defects is to reduce the overall tilt of the triclinic packing from 36° to 26°, thereby decreasing the area per molecule by 4%. The minority structure (< 10%) is a four-molecule unit cell of area 80.6 $Å^2$ (20.1 $Å^2$/molecule) in which pairs of molecules are packed in a tilted (19°) rectangular herringbone lattice, but adjacent pairs alternate vertically up and down by a single methylene group. The difference in molecular area between the two lattices is < 1%, although the details of the packing arrangement are completely different. The third structure occupies (20–30)% of the film area and is untilted but relatively disordered, but still presents diffuse spots in the Fourier transforms. The various arrangements, which are all close to the same area per molecule, are dictated by a compromise between the optimal alkane packing and the area per molecule required by the Ba^{++} counterion. Other multilayer Langmuir-Blodgett films of stearic and arachidic acids with different counterions also show that the area per molecule is primarily controlled by the counterion [8]. However, the lattice dimensions and symmetry are dictated by the close packing of the alkane chains, given the constraint of area per molecule set by the counterion. Hence, AFM studies of molecular organization of fatty-acid LB films may be ideal systems to check molecular dynamics calculations of alkane packing [13].

LB multilayers were deposited at a surface pressure of 30 mN/m on mica substrates as previously reported for CdA [6,7], using a Nima [14] trough, except that a 0.5 mM solution of $BaCl_2$ [15] (water from a Milli-Q [16] system was used), was substituted for the $CdCl_2$ and the *p*H was adjusted either to 6.9 by addition of $NaHCO_3$ or to 9.2 by addition of NaOH. We were not able to deposit multilayers at surface pressures of 10 to 20 mN/m at either *p*H, although in previous work with CdA, we observed identical lattice structures regardless of the transfer pressure [7]. AFM measurements were performed with a Nanoscope II [17] FM as previously reported [6,7].

Low-magnification images of the films (Fig. 1) show bilayer holes along with other, more subtle features. We have identified three regions with heights of 5.0 ± 0.1 nm, 5.2 ± 0.1 nm, and 5.5 ± 0.1 nm, respectively, when measured from the bottom of the bilayer holes (the monolayer is unstructured and flat, as with CdA [6,7]). A fully extended, untilted bilayer has a height of 5.5 nm [7]. Approximately sixty well-calibrated, drift-free molecular-resolution images (30–40 nm on a side) were obtained on four independent three-layer LB films (two each at *p*H = 6.9 and 9.2) using seven different AFM tips. There was perfect correlation between the molecular structures observed and the height of the region, the 5.0 nm high regions having the 3×1 structure (~70% of the surface), the 5.2 nm high regions the 2×2 structure (< 10%), and the 5.5 nm high regions the disordered structure

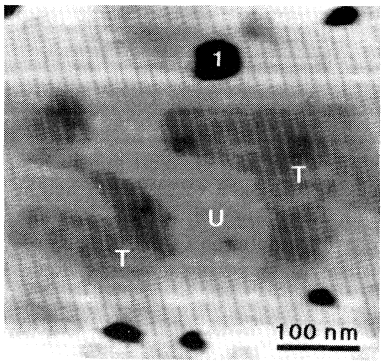

FIG. 1. Low-magnification image of a three-layer BaA LB film. Lighter colors correspond to higher regions. The surface has various regions labeled "T" for tilted, "U" for untilted, and "1" for a one-layer region at the bottom of a bilayer hole.

(~25%). We have used the nomenclature of surface reconstruction, since in both cases the surface structure is related to more familar bulk packings but with distinctive height modulations.

Although BaA films made at pH=6.9 contain only (50–60)% of the possible Ba and those made at pH > 9 have 100% Ba [18], we noticed no significant difference in our results for the two types of film. This is consistent with IR measurements that show that the alkane chains in multilayer Ba stearate are arranged in a triclinic packing that is invariant with pH from 7 to 9.5 [19]. Surface potential measurements [20] suggest that the Ba ion interacts with fatty acids electrostatically by screening negative charges in a nonspecific way, while Cd interacts more specifically via covalent bonding. Hence, BaA films are a mixture of protonated and deprotonated fatty acids with Ba over the entire pH range [19,21], while cadmium forms specific complexes with deprotonated fatty acids with a well-defined stoichiometry [11,19,20,22].

Molecular-resolution images of each structure are shown in Figs. 2(a), 2(c), and 2(e) with their two-dimensional Fourier transforms (FT) shown in Figs. 2(b), 2(d), and 2(f). The FT's of the disordered images varied spatially and temporally so no lattice structure was determined; however, positional correlations extended 5–6 repeat distances. A statistical analysis [7] was used to determine the best fit to the reciprocal lattice vectors (rlv) $\mathbf{b}_n$ for both the 3×1 and the 2×2 lattices [$\mathbf{b}_1$ and $\mathbf{b}_2$ are labeled in Figs. 2(b) and 2(d)]. The positions of the rlv's are enough to determine the unit cell dimensions which are defined by the basis vectors $\mathbf{a}_1$ and $\mathbf{a}_2$ [Figs. 3(a) and 3(c)].

For the 3×1 structure, further structural information is provided by the autocorrelation function [Fig. 4(a)], and the height modulation of the image along the [01] direction [Fig. 4(b)], which yields local packing defined by $\mathbf{a}_1$ and a second vector $\mathbf{u}$, as shown in Fig. 3(a). The positions of the three molecules within the unit cell are defined by translations of $\pm\mathbf{u}$ with a unit cell area of

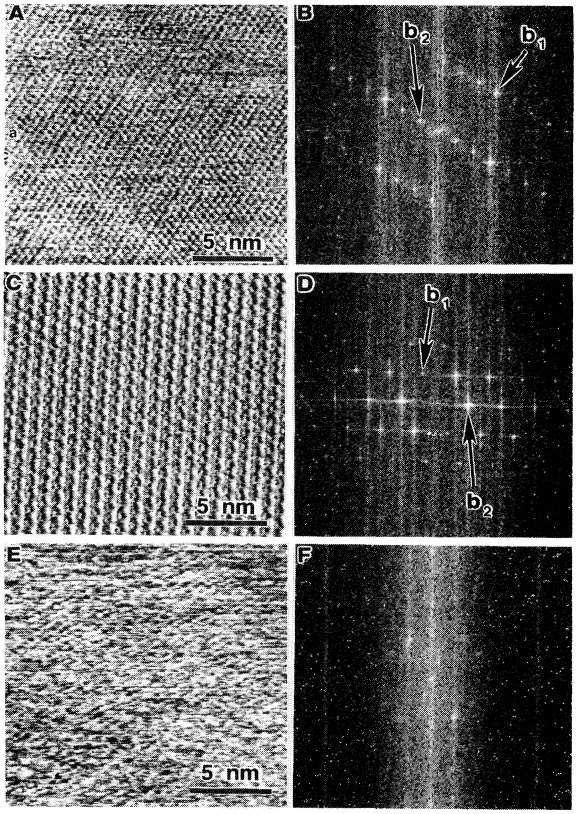

FIG. 2. Unprocessed molecular-resolution images and Fourier transforms of the various structures seen. (a) 3×1; the sawtooth superstructure is seen every three rows. (b) Fourier transform (FT) of (a) with the basis of the reciprocal lattice labeled. (c) 2×2; alternating rows of high and low molecules can be clearly seen. (d) FT of (c). (e) Disordered; isolated areas of molecular order are visible but without long-range correlation. (f) FT of (e). The peaks are diffuse due to short-range order. In all of the FT's, the vertical and horizontal streaks are due to noise generated by the discrete raster pattern of the AFM.

61.1 Å^2 (20.4 Å^2/molecule). Figure 3(b) illustrates a remarkable coincidence: The lattice vectors of the unit cell can be exactly constructed from the local packing vectors by inverting every third local cell, which corresponds to a distinct packing defect. In the height cross section taken in the [01] direction [Fig. 4(b)], one can notice a regular sawtooth pattern with a period of three molecules. This suggests that the packing defect includes a displacement in the z direction. Figure 5(a) shows a view along the alkyl chain axes of a tilted structural model (consistent with the data) formed by displacing a neighboring molecule along its axis by the repeat distance along the chain. The uniformly tilted triclinic regions on top and bottom (packed locally in what is called the "T" subcell [12]) are joined by a very specific sort of defect, similar to a stacking fault in three dimensions. If we project the lattice dimensions deduced from our experiments onto the plane

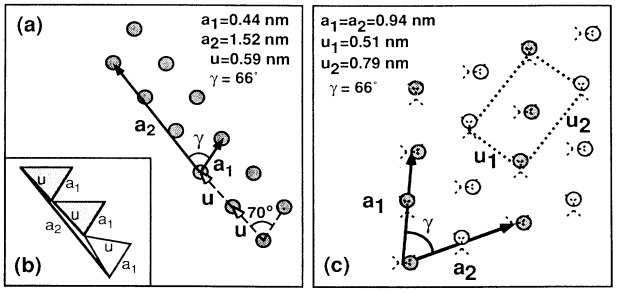

FIG. 3. (a) Unit cell diagram of the 3×1 structure showing the three-molecule unit cell dimensions $\mathbf{a}_1$ and $\mathbf{a}_2$ as well as the positions of molecules within the unit cell given by translations of $\pm\mathbf{u}$. (b) Explicit illustration of how the unit cell can be constructed by inverting every third "local cell," suggesting that a simple packing defect is inserted every three molecules. (c) Unit cell diagram of the 2×2 structure showing the unit cell dimensions $\mathbf{a}_1$ and $\mathbf{a}_2$ as well as the centered rectangular packing (defined by $\mathbf{u}_1$ and $\mathbf{u}_2$) of which the lattice is constructed. The dashed figures represent the hydrocarbon skeleton of each molecule and demonstrate the herringbone nature of local packing. The circles represent the position of the terminal methyl groups, with the light ones being displaced vertically by a chain repeat distance (2.54 Å) relative to the dark ones.

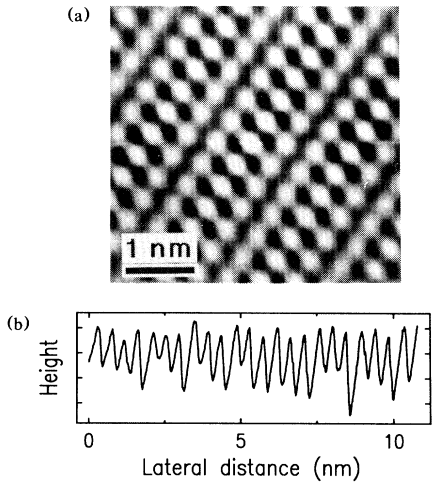

FIG. 4. (a) Two-dimensional autocorrelation function of the image shown in Fig. 1(a). Note the packing defects separating every three rows of local packing. (b) Height cross section taken in the [01] direction of an unprocessed image. The sawtooth pattern is most easily observed by noting the modulation of the depth of the troughs between molecules.

perpendicular to the alkane chains, we obtain the local chain packing dimensions $a_1^{(ch)}=0.42\pm0.01$ nm, $a_2^{(ch)}=0.45\pm0.01$ nm, with the angle between them $\gamma^{(ch)}=76°\pm1°$. This compares favorably with Kitaigorodskii's [12] ideal values of 0.412 nm, 0.445 nm, and 77° for this type of packing. The packing defect reduces the tilt to 26° from a value of 36° in the uniformly tilted structure, which is consistent with the measured bilayer heights (5.0 ± 0.1 nm) of these regions [$5.5\cos(26°)=5.05$]. IR measurements also suggest a local triclinic packing for Ba stearate [19] and x-ray-absorption fine structure suggests a similar tilt in films of calcium arachidate [23].

High-resolution images of the 2×2 structure [Fig. 6(a)] and the cross section along the $\mathbf{a}_2$ direction [Fig. 6(b)] clearly show alternate rows of low and high molecules, in addition to a zigzag pattern along the rows. These features and the lattice distances and symmetry are consistent with the type of structure shown in Figs. 3(c) and 5(b), which show the centered rectangular "herringbone" structure [6,7] tilted 19° along the $\mathbf{u}_2$ direction (Kitaigorodskii's [12] R[01]). In addition, however, every other ($\mathbf{a}_1$) row of molecules is displaced vertically by a repeat distance (2.54 Å) along the chain. The local packing dimensions calculated from this structure [Fig. 3(c)] of $\mathbf{u}_1=0.51\pm0.01$ nm, $\mathbf{u}_2=0.79\pm0.01$ nm compare favorably with the "ideal" chain packing dimensions for the tilted rectangular structure [12], of 0.496 and 0.785 nm. The calculated tilt angle is also consistent with the measured bilayer height of 5.2 ± 0.1 nm as $5.5\cos(19°)=5.26$. The molecular area of the 2×2 lattice is 80.6 Å^2 (or 20.1 Å^2/molecule); thus the difference in molecular area between the 2×2 and 3×1 structures is only 1%, although the packing arrangements are quite different.

The third structure, which occupies (20–30)% of the area of the film, is disordered in comparison to the other two areas, but still presents diffuse spots in the Fourier transforms and some evidence of rowlike patterns in the images. These disordered areas are found to be untilted by comparing the bilayer thickness of the three regions. A rough estimate of the molecular area gives a value close to that of the two lattice structures.

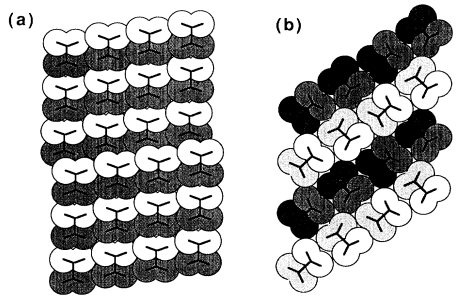

FIG. 5. Structural models of the packing of alkyl chains, viewed along the chain axis. The black lines represent the projected hydrocarbon backbone of the chain, while the circles represent the radius of the hydrogen atoms. (a) 3×1 structure. The shaded and unshaded circles represent the hydrogen atoms belonging to the even and odd carbons, respectively. The regions of tilted triclinic packing at top and bottom are separated by a packing defect (exactly every three rows) which causes a jump in the structure both vertically and in the plane. (b) 2×2 structure. The circles filled with darker colors represent molecules in rows that are displaced vertically by a chain repeat distance relative to the lighter molecules. Along each row the herringbone pattern can be seen.

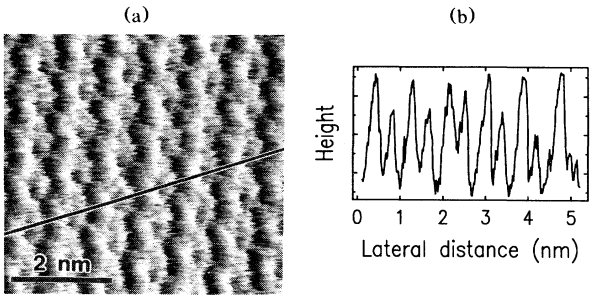

FIG. 6. (a) High-resolution image of the 2×2 structure showing the alternating rows of high and low molecules (nearly vertical) as well as the zigzag within each row which corresponds to the alternation in hydrocarbon chain orientation. (b) A height map along the line marked in (a). The alternation of low and high molecular rows can be seen. Although this picture was taken in "force" mode which does not give calibrated height information, images taken in "height" mode show the height modulation to be 0.15 ± 0.1 nm.

Bulk crystals of a given fatty acid have often been assigned different crystal symmetries when prepared by different methods [12]. At least three types of symmetry are known, *A*, *B*, and *C*. The nearly centered rectangular 2×2 structure is related to the *B* and *C* types, while the triclinic 3×1 structure is similar to the *A* type. To accommodate the Ba^{++} ion, the alkane lattice must be more loosely packed than the untilted herringbone structure observed in CdA [6,7], and so must tilt by introducing a regular offset of one or more methylene groups per chain leading to a reduction in the alkane-alkane contact, and a consequent reduction in the van der Waals interaction energy. This reduction in intermolecular cohesion might be responsible for our inability to transfer BaA films at lower surface pressures. The appearance of regular defects may be a compromise between the two driving forces. The 3×1 structure is favored, perhaps because it allows more alkane contact, but not so much as to eliminate other structures.

We have also observed regular, periodic height modulations in films of CdA [6,7] and manganese arachidate (MnA) [8]. A typical peak to valley height was ≤ 0.1 nm, significantly less than the vertical offsets in the BaA lattices. The modulation wavelength was 1.9 ± 0.3 nm along the [01] direction of every film we examined for cadmium with fatty acids of chain length C_{16} to C_{20}. (The unit cell for both Cd and Mn films was rectangular with a two-molecule basis; however, Cd is untilted with a molecular area of 18 $Å^2$ and Mn is tilted 19° with a molecular area of 19.6 $Å^2$ [6-8]). The modulation in CdA does not appear commensurate, and varies from domain to domain. Three-layer films of MnA also have a superstructure along the [01] direction with a wavelength of 1.18 ± 0.08 nm, considerably less than that in the cadmium films. The period of the buckling on MnA is much better defined and is close to commensurate [8]. We postulated previously [6] that the superstructures observed in CdA and MnA are related to packing frustration due to the internal anisotropy of the molecule [24]. In particular, there may be a competition between the packing of the head and tail groups due to different size or symmetry. Preliminary images of calcium arachidate films also show regions of different height, although there does not seem to be the simple correlation between the local lattice structure and the bilayer thickness as in BaA.

This work was supported by the Office of Naval Research under Grant No. N00014-90-J-1551, the National Science Foundation under Grant No. CTS90-15537, the National Institutes of Health under Grant No. GM 47334, and the Donors of the Petroleum Research Foundation.

[a]To whom correspondence should be addressed. Phone: (805) 893-4769. FAX: (805) 893-4731. Electronic address: gorilla@squid.ucsb.edu

[1] G. G. Roberts, Adv. Phys. **34**, 475 (1985).
[2] See Ref. [6] for an extensive reference list.
[3] G. Binnig, C. F. Quate, and Ch. Gerber, Phys. Rev. Lett. **56**, 930 (1986).
[4] M. Egger *et al.*, J. Struct. Bio. **103**, 89 (1990); J. A. N. Zasadzinski *et al.*, Biophys. J. **59**, 755 (1991).
[5] E. Meyer *et al.*, Nature (London) **349**, 398 (1991).
[6] J. Garnaes *et al.*, Nature (London) **357**, 54 (1992).
[7] D. K. Schwartz *et al.*, Science **257**, 508 (1992); D. K. Schwartz *et al.*, Phys. Rev. E **47**, 452 (1993).
[8] D. K. Schwartz *et al.*, "Influence of Cations and Alkane Chain Length on Molecular Order of Langmuir-Blodgett Films," (to be published).
[9] H. G. Hansma *et al.*, Langmuir **7**, 1051 (1991); R. Viswanathan *et al.*, Langmuir **8**, 1603 (1992).
[10] D. K. Schwartz, R. Viswanathan, and J. A. N. Zasadzinski, J. Phys. Chem. (to be published).
[11] F. Leveiller *et al.*, Science **252**, 1532 (1991); M. L. Schlossman *et al.*, Phys. Rev. Lett. **66**, 1599 (1991).
[12] A. I. Kitaigorodskii, *Organic Chemical Crystallography* (Consultant Bureau, New York, 1961).
[13] S. Karaborni, S. Toxvaerd, and O. H. Olsen, J. Chem. Phys. **96**, 4965 (1992); J. P. Bareman, G. Cardini, and M. L. Klein, Phys. Rev. Lett. **60**, 2152 (1988).
[14] NIMA Technology Ltd., Warwick Science Park, Coventry, CV4 7EZ, England.
[15] Aldrich Chemical Co., Milwaukee, WI.
[16] Millipore Corp., Bedford, MA.
[17] Digital Instruments, Inc., Goleta, CA.
[18] K. Kobayashi, K. Takoaka, and S. Ochiai, Thin Solid Films **159**, 267 (1988).
[19] C. Vogel, J. Corset, and M. Dupeyrat, J. Chim. Phys. **76**, 909 (1979).
[20] M. Yazdanian, H. Yu, and G. Zografi, Langmuir **6**, 1093 (1990).
[21] G. Bolbach *et al.*, Thin Solid Films **210/211**, 524 (1992).
[22] J. Daillant *et al.*, Langmuir **7**, 611 (1991).
[23] D. A. Outka *et al.*, Phys. Rev. Lett. **59**, 1321 (1987).
[24] J. M. Carlson and J. P. Sethna, Phys. Rev. A **36**, 3359 (1987); S. A. Safran, M. O. Robbins, and S. Garoff, Phys. Rev. A **33**, 2186 (1986).

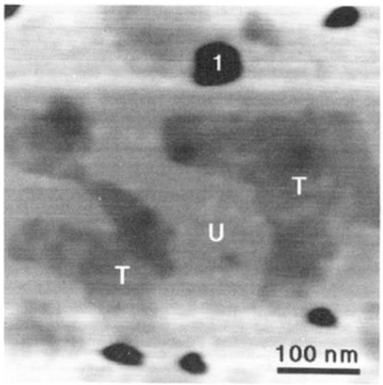

FIG. 1. Low-magnification image of a three-layer BaA LB film. Lighter colors correspond to higher regions. The surface has various regions labeled "T" for tilted, "U" for untilted, and "1" for a one-layer region at the bottom of a bilayer hole.

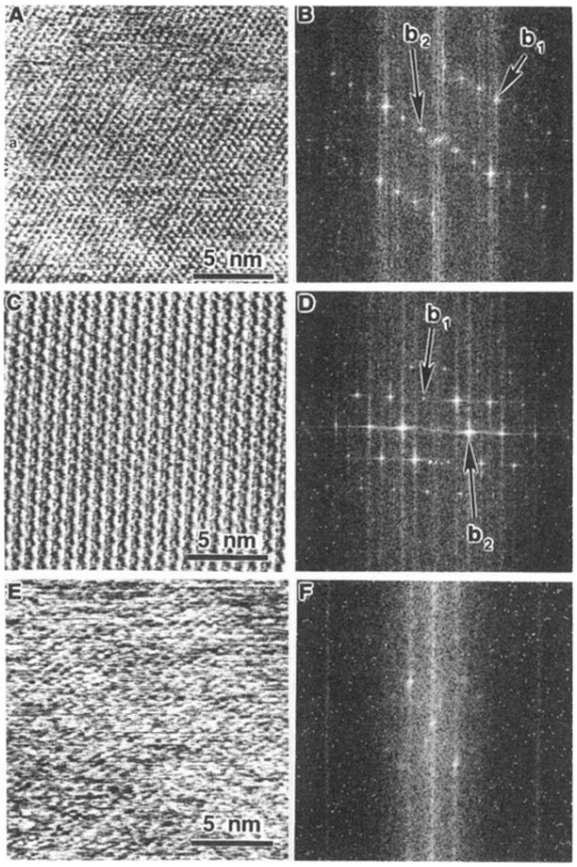

FIG. 2. Unprocessed molecular-resolution images and Fourier transforms of the various structures seen. (a) 3×1; the sawtooth superstructure is seen every three rows. (b) Fourier transform (FT) of (a) with the basis of the reciprocal lattice labeled. (c) 2×2; alternating rows of high and low molecules can be clearly seen. (d) FT of (c). (e) Disordered; isolated areas of molecular order are visible but without long-range correlation. (f) FT of (e). The peaks are diffuse due to short-range order. In all of the FT's, the vertical and horizontal streaks are due to noise generated by the discrete raster pattern of the AFM.

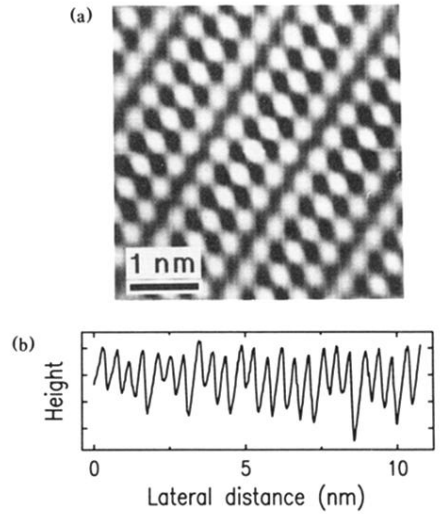

FIG. 4. (a) Two-dimensional autocorrelation function of the image shown in Fig. 1(a). Note the packing defects separating every three rows of local packing. (b) Height cross section taken in the [01] direction of an unprocessed image. The sawtooth pattern is most easily observed by noting the modulation of the depth of the troughs between molecules.

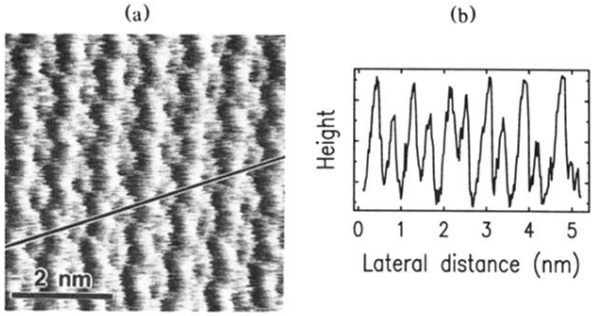

FIG. 6. (a) High-resolution image of the 2×2 structure showing the alternating rows of high and low molecules (nearly vertical) as well as the zigzag within each row which corresponds to the alternation in hydrocarbon chain orientation. (b) A height map along the line marked in (a). The alternation of low and high molecular rows can be seen. Although this picture was taken in "force" mode which does not give calibrated height information, images taken in "height" mode show the height modulation to be 0.15 ± 0.1 nm.